Matthews, D. A., Bolin, J. T., Burridge, J. M., Filman, D. J., Volz, K. W., Kaufman, B. T., Beddell, C. R., Champness, J. N., Stammers, D. K., & Kraut, J. (1985) *J. Biol. Chem. 260*, 381-391.

Morrison, J. F., & Stone, S. R. (1988) *Biochemistry 27*, 5499-5506.

Perahia, D., Pullman, B., & Saran, A. (1975) in *Structure and Conformation of Nucleic Acids and Protein-Nucleic Acid Interactions* (Sundadlingam, M., & Rao, S. T., Eds.) pp 685-708, University Park Press, Baltimore.

Rossmann, M. G., & Argos, P. (1975) *J. Biol. Chem. 250*, 7525-7532.

Sussman, J. L., Holbrook, S. R., Church, G. M., & Kim, S.-H. (1977) *Acta Crystallogr. A33*, 800-804.

Tanaka, N. (1977) *Acta Crystallogr. A33*, 191-193.

Villafranca, J. E., Howell, E. E., Voet, D. H., Strobel, M. S., Ogden, R. C., Abelson, J. N., & Kraut, J. (1983) *Science 222*, 782-788.

Volz, K. W., Matthews, D. A., Alden, R. A., Freer, S. T., Hansch, C., Kaufman, B. T., & Kraut, J. (1982) *J. Biol. Chem. 257*, 2528-2536.

Wang, J., Mauro, J. M., Fishel, L. A., Edwards, S. L., Xuong, N.-H., Ashford, V., & Kraut, J. (1990) *Biochemistry* (in press).

Wu, Y.-D., & Houk, K. N. (1987) *J. Am. Chem. Soc. 109*, 2226-2227.

Xuong, N.-H., Neilson, C., Hamlin, R., & Anderson, D. H. (1985) *J. Appl. Crystallogr. 18*, 342-350.

^{1}H NMR Sequential Assignments and Secondary Structure Analysis of Human Fibrinogen γ-Chain C-Terminal Residues 385-411†

K. H. Mayo* and C. Burke

Department of Chemistry, Temple University, Philadelphia, Pennsylvania 19122

J. N. Lindon

Beth Israel Hospital, Harvard Medical School, Boston, Massachusetts 02155

M. Kloczewiak

Burns Institute, Shriners Hospital for Crippled Children, Boston, Massachusetts 02114

Received August 1, 1989; Revised Manuscript Received November 1, 1989

ABSTRACT: The human fibrinogen γ-chain, C-terminal fragment, residues 385-411, i.e., KIIPFNRLTIGEGQQHHLGGAKQAGDV, contains two biologically important functional domains: (1) fibrinogen γ-chain polymerization center and (2) platelet receptor recognition domain. This peptide was isolated from cyanogen bromide degraded human fibrinogen and was investigated by ^{1}H NMR (500 MHz) spectroscopy. Sequence-specific assignments of NMR resonances were obtained for backbone and side-chain protons via analysis of 2D NMR COSY, double quantum filtered COSY, HOHAHA, and NOESY spectra. The N-terminal segment from residues 385-403 seems to adopt a relatively fixed solution conformation. Strong sequential αCH-NH NOESY connectivities and a continuous run of NH-NH NOESY connectivities and several long-lived backbone NH protons strongly suggest the presence of multiple-turn or helix-like structure for residues 390 to about 402. The conformation of residues 403-411 seems to be much less constrained as evidenced by the presence of weaker and sequential αCH-NH NOEs, the absence of sequential NH-NH NOEs, and the lack of longer lived amides. Chemical shifts of resonances from backbone and side-chain protons of the C-terminal dodecapeptide, residues 400-411, differ significantly from those of the parent chain, suggesting that some preferred C-terminal conformation does exist.

The vertebrate fibrinogen molecule (330000 daltons) in its native form is a dimer, each half-molecule being composed of three nonidentical polypeptide chains (α, β, and γ) (Blomback & Yamashina, 1958). Its transformation into fibrin is a self-assembly process following thrombin-catalyzed removal of fibrinopeptides from the amino termini of the α- and β-chains. The fibrinogen chains can be chemically cross-linked between two α-chains (McKee et al., 1970) and between two γ-chains (Chen & Doolittle, 1969), presumably through ε-amino(γ-glutamyl)lysine bonds (Chen & Doolittle, 1970). The C-terminal γ-chain fragment of residues 392-411 was identified as being responsible for the γ-γ chain cross-linking/polymerization (Chen & Doolittle, 1971). Doolittle (1973) modeled this segment in an α-helix structure to hypothesize cross-linking sites between γ-chains.

More recently, Kloczewiak et al. (1982) showed that the domain recognizing receptors on ADP-activated human platelets is located on the human fibrinogen γ-chain between residues 385 and 411 which when cleaved to the smaller fragment, residues 400-411, maintains nearly full biological activity (Kloczewiak et al., 1984). Substitution of one amino acid for another in this dodecapeptide fragment can greatly affect its activity (Ruggeri et al., 1986; Kloczewiak et al., 1988), suggesting that either a specific (sequence of) residue(s) or a specific backbone folding pattern or both is necessary for activity.

Due to the biological significance of the fibrinogen γ-chain C-terminal fragment, we chose to investigate the solution conformation of γ-chain residues 385-411 by using two-dimensional (2D)[1] proton NMR spectroscopy. In this study,

†This work was supported by a grant from the W. W. Smith Charitable Trust and benefited from NMR facilities made available to Temple University through Grant RR-04040 from the National Institutes of Health (to K.H.M.).

*Author to whom correspondence should be addressed.

0006-2960/90/0429-3277$02.50/0

we present sequential proton resonance assignments and secondary structure elements.

Materials and Methods

Human fibrinogen (Kabi, Sweden) was used without any further purification. Preparation of carboxymethylated γ-chain, degradation of the γ-chain with cyanogen bromide, and gel filtration chromatography of the γ-chain fragments on Sephadex G-50 columns were carried out as previously described (Kloczewiak et al., 1982) by using a Vydac C18, 300-Å, 1 × 25 cm column. A linear acetonitrile gradient from 5 to 40% was used in all runs; 0.05% trifluoroacetic acid was added to both the water and acetonitrile reservoirs. The desired peptide was eluted at approximately 12% acetonitrile and was concentrated by freeze-drying. The concentration was determined by standard amino acid analysis of the sample hydrolyzed with 6 N HCl at 150 °C for 40 min. Identity of the peptide was confirmed by amino acid analysis and amino-terminal sequencing (gas phase; Applied Bioscience automatic sequencer).

The γ-chain C-terminal fragment, residues 400–411, was synthesized by solid-phase methods (Barany & Merrifield, 1980) with a Biosearch 9500 peptide synthesizer. Peptides were cleaved from the resin with hydrofluoric acid and purified by using liquid chromatography and HPLC according to procedures described by Kloczewiak et al. (1984).

Freeze-dried samples for NMR measurements were dissolved either in D_2O or in H_2O/D_2O (9:1) at a protein concentration of about 5 mM in 20 mM potassium phosphate, pH 3. For most experiments, the temperature was controlled at 303 K. All NMR spectra were acquired on a GN-Omega-500 spectrometer equipped with a Sun-3/160 computer.

For sequential assignments, COSY (Aue et al., 1976; Wider et al., 1984), double quantum filtered COSY (Piantini et al., 1982; Shaka & Freeman, 1983), and NOESY (Jeener et al., 1979; Wider et al., 1984) experiments were performed. 2D homonuclear magnetization transfer (HOHAHA) spectra, used to identify many spin systems completely, were obtained by spin-locking with a MLEV-17 sequence (Davis & Bax, 1985) with a mixing time of 64 ms. All but the COSY spectra were acquired in the phase-sensitive mode (States et al., 1982). The water resonance was suppressed by direct irradiation (1 s) at the water frequency during the relaxation delay between scans as well as during the mixing time in NOESY experiments.

The majority of the 2D NMR spectra were collected as 512 or 1024 t_1 experiments, each with 2K complex data points over a spectral width of 5 kHz in both dimensions, with the carrier placed on the water resonance. A total of 64 or 96 scans were generally time-averaged per t_1 experiment. The data were processed directly on the Sun-3/160 computer. Data sets were multiplied in both dimensions by a 0–60°-shifted sine-bell or Lorentzian or Gaussian transformation function and generally zero-filled to 1K in the t_1 dimension prior to Fourier transformation.

The relative exchange rates of amide protons were qualitatively determined by following the kinetics of proton–deuteron exchange. Normally, the H_2O-exchanged, lyophilized peptide was dissolved in D_2O/20 mM potassium phosphate, pH 3, at 0 °C and then allowed to equilibrate in the spectrometer at 25 °C before acquiring the first spectrum. Residual NH signal intensities were followed with time. Many amide protons exchanged within seconds or minutes, while a number were relatively long-lived, i.e., half-life about 30 min. Ambiguities due to NH resonance overlap were removed for the longest lived amides by recording a COSY spectrum in D_2O at 10 °C where exchange rates are attenuated.

Results

Resonance Assignments. Spin system assignments were made primarily on the basis of COSY and HOHAHA spectra analysis. A COSY contour plot of FGC 385–411 in D_2O (Figure 1) allows tentative partial resonance identification of the unique T393 and P388 spin systems. In particular, the P388 δ,δ′CH resonances are well separated by 0.2 ppm which is probably the result of proximity to the F389 ring and perhaps a fixed backbone conformation. The more deshielding P388 δCH resonance is downfield-shifted by about 0.25 ppm relative to its random-coil position (Bundi & Wüthrich, 1979). A tentative unique valine (411) spin system assignment could also be made since its αCH, βCH_2, and γCH_3 resonance connectivities could be easily followed. The five AMX spin systems, i.e., F389, N390, H400, H401, and D410, were also identified, as were the two alanine (405 and 408) and four glutamate/glutamine (396, 398, 399, and 407) spin systems. The five glycine αCH_2 resonances are bunched up around 4 ppm. These initial assignments have been identified in Figure 1.

A HOHAHA contour plot (Figure 2) allowed more complete spin system identifications. In this experiment, total J correlation from NH through terminal side-chain CH resonances could be made for most spin systems with the exception of the N-terminal K385 in the fragment. Comparing the HOHAHA spectrum with that of the COSY spectrum (Figure 1) confirms the unique T393 and V411 assignments. The five AMX and five glycine spin systems were easily singled out. The well-resolved γCH_2 resonances of the four glutamate/glutamine spin systems allowed clear identification of their individual αCH and βCH_2 resonances from the COSY spectrum. The five remaining aliphatic, hydrophobic spin systems (two leucine and three isoleucine) were, as a group, identified in the HOHAHA spectrum through their upfield methyl resonances. Specific assignments given in Figure 2 were the result of sequential resonance assignments shown in the NOE map (Figure 3).

The tracing from K385 through G395 in Figure 3 is unambiguous. Starting from P388, one can proceed in either direction. To the C-terminal side, the P388 αCH shows a strong cross-peak to the F389 NH. This αCH_i to NH_{i+1} jumping pattern can be followed to the NH of G395. The NH of the unique T393 residue gives a cross-peak to the αCH of L392 whose NH is NOESY connected to the αCH of R391. The αCH of T393 can also be followed through to the NH of G395 on its C-terminal side. The δ,δ′CH protons of P388 give strong NOESY cross-peaks (Figure 4) to the αCH of their N-terminal neighbor, I387. The NH of I387 can then be clearly traced through to the αCH of K385. The K385 αCH–NH cross-peak is absent in the J-correlated spectrum (Figure 2) most likely due to rapid solvent exchange of its terminal backbone NH_2 protons.

Since all five glycine αCH_2 protons resonate near 4 ppm, following the NOE map from G395 to its C-terminal neighbor was not without difficulty. Fortunately, glycine NH resonances are generally well dispersed. A clear cross-peak between a glutamate/glutamine αCH and a glycine NH iden-

[1] Abbreviations: FGC, fibrinogen γ-chain; TSP, sodium 3-(trimethylsilyl)-1-propanesulfonate; NOE, nuclear Overhauser effect; 2D NMR, two-dimensional nuclear magnetic resonance; NOESY, two-dimensional nuclear Overhauser effect spectroscopy; COSY, two-dimensional scalar correlated spectroscopy; HOHAHA, two-dimensional homonuclear magnetization transfer spectroscopy (HOmonuclear HArtmann HAhn); FID, free induction decay; HPLC, high-performance liquid chromatography; ppm, parts per million; one-letter codes for amino acids have been used when referring to sequence-specific residues.

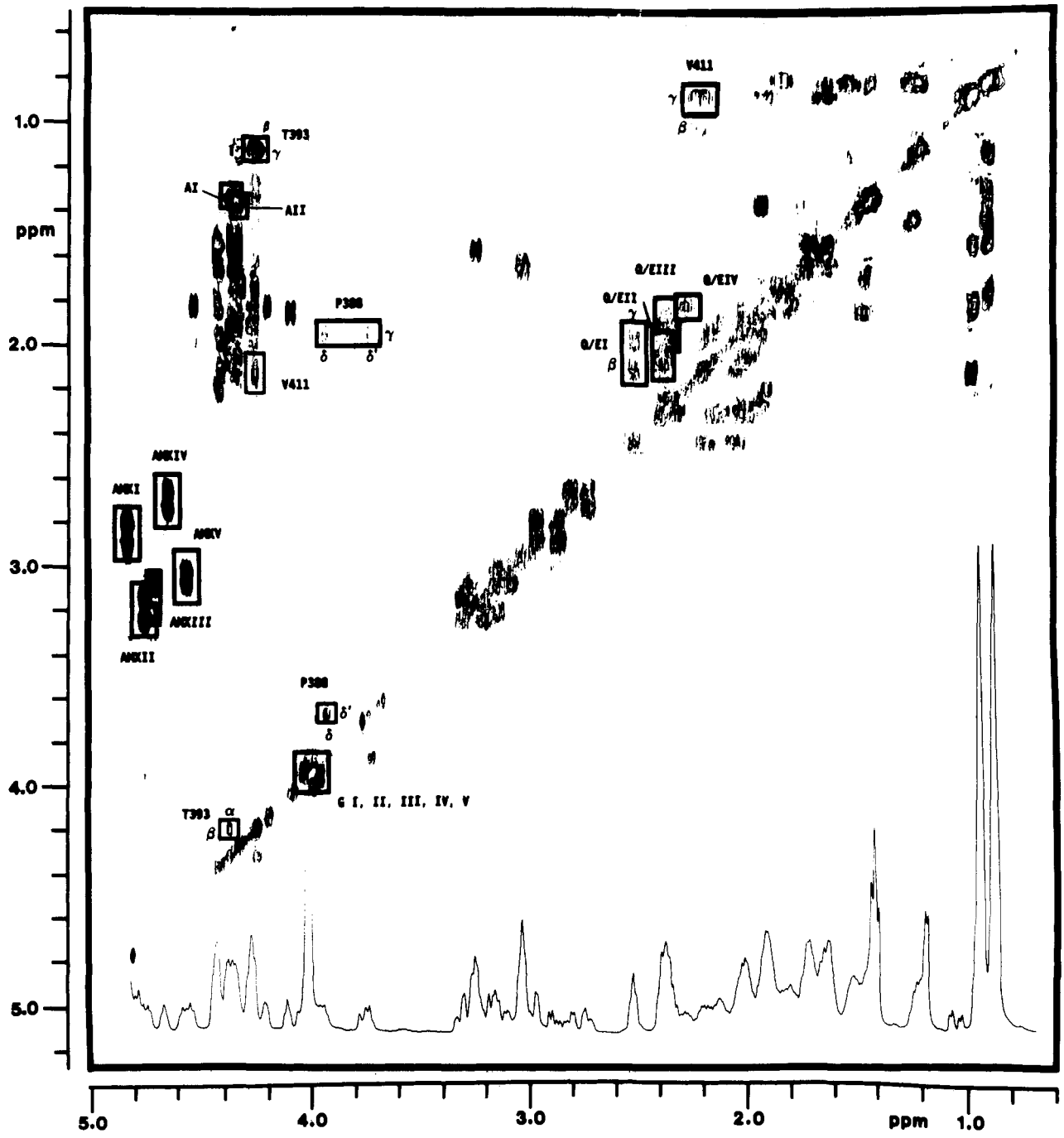

FIGURE 1: COSY contour plot of FGC 385–411. The upfield region of a 2D NMR (500 MHz) COSY contour plot of FGC 385–411 (5 mM) in D_2O/20 mM potassium phosphate, pH 3.0, 303 K, is shown. The data set was collected as 512 t_1 time incremented 2K data point FIDs and processed with a 60°-shifted sine function prior to Fourier transformation. As discussed in the text, tentatively identified cross-peaks have been boxed and labeled. A conventional proton NMR spectrum of FGC 385–411 is shown at the bottom of the figure.

tified the unique dipeptide E396-G397. The L402-G403 and A408-G409 assignments were similarly made. G404 was primarily identified by a process of elimination due mainly to overlap of the G404 and D410 NH resonances. The G397 αCH_2/Q398 NH, G395 αCH_2/E396 NH, and G404 αCH_2/A405 NH NOESY cross-peaks partially overlap near 4.0 (F1) and 8.2 (F2) ppm. The tracing from Q398 to G403 proceeded in a straightforward manner. Some cross-peaks not apparent in these data set were identified in others; their αCH–NH cross-peak positions have been indicated in Figure 3.

For the remaining sequential assignments, more ambiguities would have arisen if not for the fact that three of the eight as yet unassigned residues were unique, i.e., V411, D410, and Q407 by elimination, and two others were alanine residues. A connection from G403 to G404 could not be made unambiguously. The dipeptide sequence Q407-A408 was, however, clearly assigned. The only remaining A405 αCH, moreover, did give a small NOE to the NH of K406. Having made that assignment, a cross-peak could be identified between A408 and G409. Unfortunately, no cross-peak could be observed between D410 αCH and V411 NH due to overlap of the alanine αCH resonance with the saturated H_2O resonance. Both, however, had already been independently assigned. Some assignment confirmations were made, and ambiguities due to cross-peak overlap were clarified by acquiring spectra at slightly higher and lower temperatures. The F389, H400, and H401 resonance assignments were confirmed by intraresidue ring proton NOEs to αCH and βCH_2 resonances (data not shown). All known backbone and side-chain assignments are listed in Table I along with difference values from their random-coil chemical shift positions (Bundi & Wüthrich,

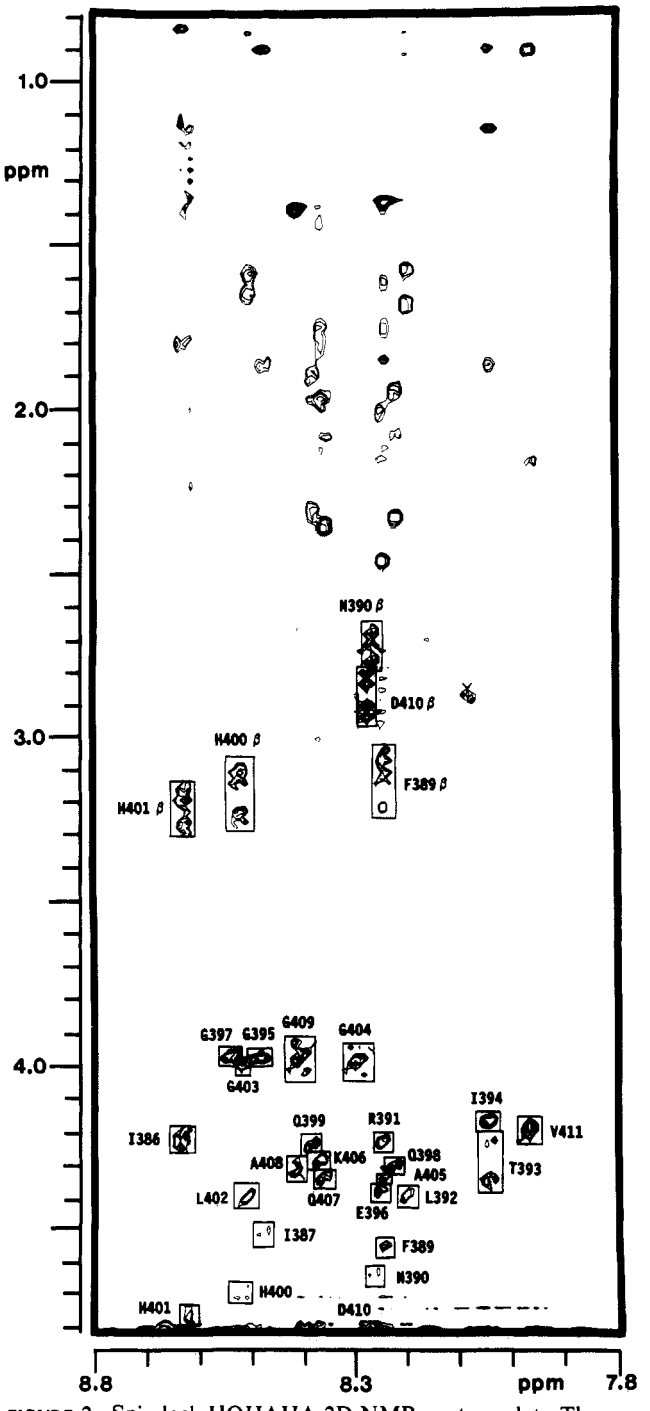

FIGURE 2: Spin lock HOHAHA 2D NMR contour plot. The amide–αCH and upfield region of a contour plot is shown for FGC 385–411. The sample concentration was 5 mM in 20 mM potassium phosphate, pH 3.0, 303 K, in H_2O (90% H_2O/10% D_2O) whose resonance was suppressed by direct saturation for 1 s prior to the preparation pulse. The data set was collected as 1024 hypercomplex FIDs containing 2K words and was processed on a Sun-3/160 computer. The data set was zero-filled to 1024 in t_1. The raw data were then multiplied by a 30°-shifted sine-squared function in t_1 and t_2 prior to Fourier transformation. Labeling of resonances is as described in the text.

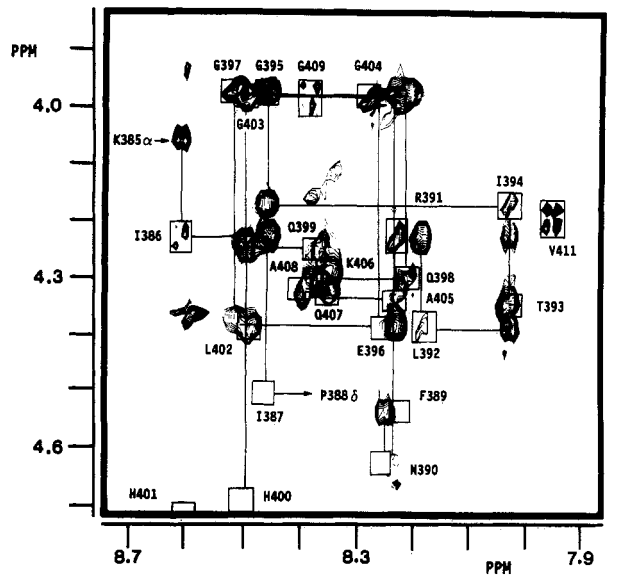

FIGURE 3: NOE map of FGC 385–411. The backbone amide–αCH region of a NOESY contour plot has been correlated with information from a COSY experiment to exemplify sequential resonance assignments. The NOESY mixing time was 200 ms. Solution conditions are as described in the Figure 2 legend. Labeling of resonances is as described in the text and has been done for most of the NOESY cross-peaks in this composite. COSY cross-peak positions are boxed and are indicated by residue number. The data set was collected as 1024 hypercomplex FIDs containing 2K words and then zero-filled to 1K in the t_1 dimension and multiplied by a Lorentzian to Gaussian transformation function prior to Fourier transformation. A conventional proton NMR spectrum is shown at the top of the figure.

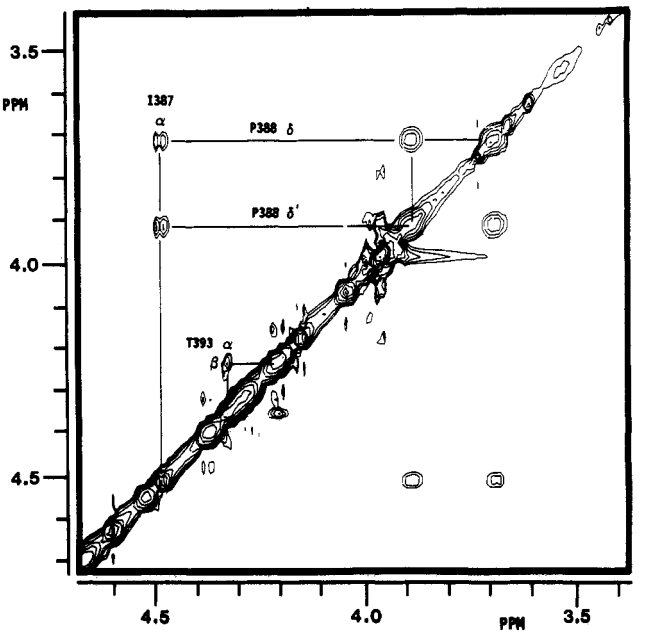

FIGURE 4: NOESY contour plot of the αCH region. The αCH region of a NOESY contour plot is shown for FGC 385–411 in D_2O under conditions as described in the Figure 2 legend. The data were acquired and processed as described in the Figure 2 legend.

1979). All NMR analyses were done at pH 3 for two reasons: (1) greater peptide solubility and (2) amide proton exchange rates. As the pH was raised to 4 and above, 5 mM FGC 385–411 slowly precipitated on standing. Moreover, above pH 5, even when the peptide remained in solution at lower concentrations, NH resonance intensities in H_2O were greatly attenuated due to increased rates of exchange. Raising the pH from 3 to 7 is expected to affect protonation states for H400, H401, and perhaps E396 and D410, and thereby maybe affect structural stability if, for example, these residues were involved in electrostatic interactions. It should be mentioned that most proteins studied to date by 2D NMR methodology have been investigated at similar nonphysiological pH values for the same reasons mentioned above (Wüthrich, 1986).

Secondary Structure Elements. The NH to NH NOESY spectral region is shown in Figure 5. A number of d_{NN} cross-peaks are present which run continuously from I394 through H400. Two other cross-peaks exist between L392 and T393, and between H401 and L402. These and other

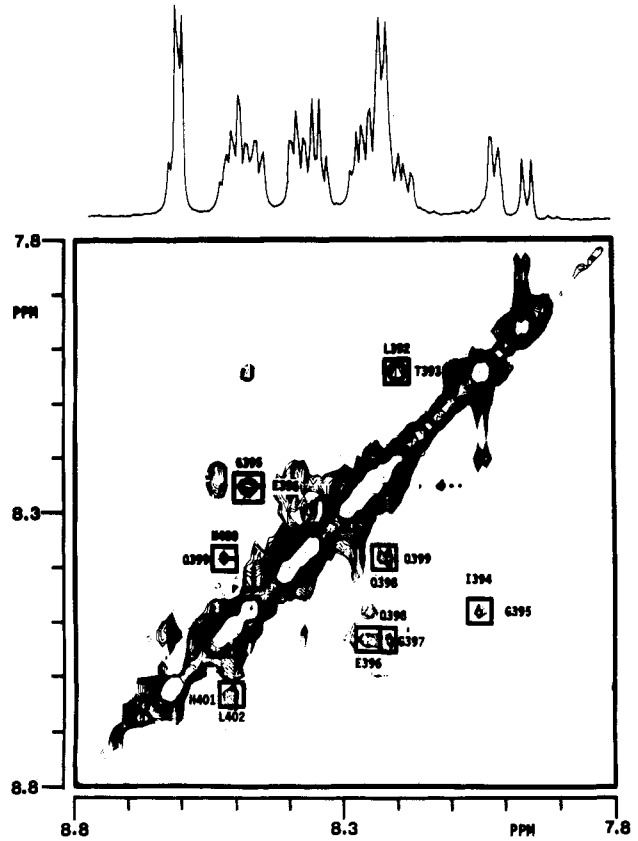

FIGURE 5: NH–NH cross-peak region. The downfield region of a NOESY contour plot (mixing time, 300 ms) is shown for FGC 385–411. The experimental and data processing conditions are as described in the Figure 2 legend.

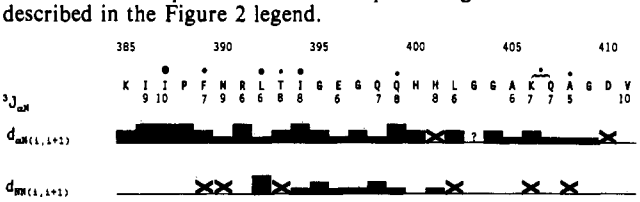

FIGURE 6: Amino acid sequence of FGC 385–411 and survey of NMR data used for locating secondary structure. The amino acid sequence of FGC 385–411 is shown using one-letter codes. The NMR data are compiled from NOESY spectra acquired using short and long mixing times of up to 400 ms. The NOEs, relatively classified as weak, medium, and strong, are represented by the thickness of the bars. $J_{NH-\alpha CH}$ coupling constants, taken from double quantum filtered COSY data, are also given. Long-lived backbone amide protons are indicated by solid circles above the amino acid sequence; the size of the circles indicates the relative lifetime (i.e., larger means longer). Cross-peaks too close to the diagonal to be observed are indicated by an "X", and ambiguous cross-peaks are indicated by a "?".

NOE/NMR data are summarized in Figure 6 along with $^3J_{\alpha NH}$ coupling constants which were estimated from a double quantum filtered COSY spectrum.

Dominant solution structures for small peptides are often not found; rather, such peptides exist in a multitude of fluctuating conformational substates. Highly fluctuating peptide structures in NMR experiments are generally characterized by $^3J_{\alpha N}$ coupling constants of 6.5–8 Hz (Kessler & Bermel, 1986) and by weak or absent short-range $d_{\alpha N}$ and d_{NN} NOEs. The magnitude of an NOE depends on a number of variables which include the experimental 2D NMR mixing time, the motional properties of the spin system in question, the resonance frequency of the spectrometer, and the inverse sixth power of the distances separating pairs of spins. An analysis of any such effects can be quite involved as a rigorous treatment requires consideration of a highly coupled set of cross-relaxation interactions as well as a detailed model for molecular interactions [see Wüthrich (1986) and references cited therein]. Moreover, for small peptides, NOEs normally tend to approach zero or more positive values since the product of the Larmor precession frequency and the spin's overall correlation time tends toward unity. Effectively, this means that maximal observable distances will be in the range of about 3–4 Å instead of the usually cited 4–5-Å distance cutoff observed in larger and/or more structurally constrained proteins (Wüthrich, 1986). If we assume a two-spin model as a first approximation, we can semiquantitatively relate the magnitude of an NOE and its internuclear distance (Dobson et al., 1980). For this argument, distances and NOE magnitudes can be normalized against the P388 δCH–δCH NOE (Figure 4) where the interproton distance is fixed at 1.5 Å. It must be assumed, however, that the average correlation time for other backbone protons is the same as that for P388 δCH protons. If anything, overall correlation times would be smaller for other backbone protons and fractional NOEs would tend to be smaller than predicted. If we take a typical, extended-chain $d_{\alpha N}$ distance of closest approach, 2.2 Å, and an opposing rotomer population distance of furthest approach, 3.6 Å, we can estimate an average, harmonically oscillating, rotomer population distance of about 2.9 Å. Estimating NOE magnitudes by normalizing these distances against the observed P388 δCH–δCH fractional NOE of 0.3, $d_{\alpha N}$ fractional NOEs should be about 0.02–0.05 at 2.2 Å, about 0.005 at 2.8 Å, and much less than 0.005 at 3.6 Å. Most of the $d_{\alpha N}$ NOEs which are observed for residues 385–403 are in the 0.02–0.05 range. A similar argument can be made for observed d_{NN} NOEs. Here, the d_{NN} distance for a β-turn and α-helix conformation is about 2.4 and 2.8 Å, respectively. The alternative, furthest approach distance of an extended-chain conformation is about 4.4 Å which would be expected to show no representative d_{NN} NOE. The average rotomer population distance is about 3.3 Å. The observed d_{NN} NOEs are about 0.01. Therefore, the average rotomer population must be weighted toward the conformation of closest approach or to a limited number of similar conformations in each case. These observations are consistent with the idea of a preferred solution conformation for at least the N-terminal segment, i.e., residues 385–403, of FGC 385–411.

The presence of strong backbone NH–αCH NOESY cross-peaks between K385 and I386 and between I386 and I387 with $^3J_{\alpha NH}$ coupling constants of 9–10 Hz for I386 and I387 indicates a short N-terminal, extended-chain segment from K385 to I387. Due to the presence of large NOEs between the I387 αCH and P388 δ,δ′CHs (Figure 4), the trans proline conformation is the more favored one (Wüthrich, 1986). Moreover, the magnitude of these NOEs suggests that the average conformation places the I387 αCH equidistant from both P388 δCH protons. The P388 αCH gives a large NOE to the F389 NH in further support of a trans proline conformation. These conformational parameters define a backbone "kink" at P388. Overlap of the N390 and F389 NH resonances prohibits observation of a possible NOESY NH–NH cross-peak and eliminates possible evidence for a complete turn at P388.

Another short extended-chain segment runs from F389 to R391 as evidenced by the presence of large αCH to NH NOEs and a 9-Hz $^3J_{\alpha N}$ coupling constant for N390. This segment breaks into a probable turn at R391 with L392 and T393 in turn positions 3 and 4. This is supported by two observations: (1) a strong $d_{\alpha N}$ NOE between R391 and L392 and (2) a strong d_{NN} NOE between T393 and L392. These structural elements are suggestive of a β-turn, but the normally observed

Table I: ^{1}H NMR Sequence Assignments of the γ-Chain of Fibrinogen[a]

residue	NH	NH–nsp[b]	αCH	α–nsp[b]	βCH	β–nsp[b]	others
Lys-385	?		4.10	−0.26	1.91	+0.06	γCH 1.43, 1.43
					1.91	+0.15	δCH 1.72, 1.72
							εCH 3.03, 3.03
							εNH 7.62
Ile-386	8.62	+0.43	4.22	−0.01	1.82	−0.08	γCH 1.42, 1.15
							γCH 0.95
							δCH 0.84
Ile-387	8.46	+0.27	4.51	−0.28	1.87	−0.03	γCH 1.50, 1.18
							γCH 0.90
							δCH 0.85
Pro-388			4.40	−0.04	2.26	−0.02	γCH 2.03, 2.03
					1.88	−0.14	δCH 3.92, 3.71
Phe-389	8.21	−0.02	4.54	+0.05	3.11	−0.11	3,5H 7.33
					3.07	+0.08	2,6H 7.24
							4H 7.29
Asn-390	8.24	−0.51	4.64	−0.12	2.77	−0.06	
					2.70	−0.05	
Arg-391	8.27	0	4.24	−0.14	1.87	0	γCH 1.62
					1.77	0	δCH 3.22
							ωNH 7.25
Leu-392	8.19	−0.23	4.40	+0.02	1.69	+0.04	δCH 0.92, 0.85
					1.59	−0.06	γCH 1.69
Thr-393	8.00	−0.24	4.33	−0.02	4.24	+0.02	γCH 1.17
Ile-394	8.01	−0.18	4.15	−0.08	1.59	−0.31	γCH 1.47, 1.20
							γCH 0.99
							δCH 0.94
Gly-395	8.47	+0.08	3.96	+0.01			
			3.96	+0.01			
Glu-396	8.25	−0.12	4.37	+0.08	2.16	+0.07	γCH 2.47
					2.01	+0.04	
Gly-397	8.55	+0.16	3.97	+0.02			
			3.97	+0.02			
Gln-398	8.21	−0.02	4.30	−0.07	2.10	−0.03	γCH 2.33
					1.95	−0.06	δNH (7.45), 6.83
Gln-399	8.37	−0.04	4.23	−0.14	1.90	−0.23	γCH 2.31
					1.90	−0.11	δNH (7.51), 6.83
His-400	8.50	+0.09	4.62	+0.06	3.26	0	4H 7.32
					3.15	−0.05	2H 8.67
His-401	8.60	+0.19	4.69	−0.01	3.27	+0.01	4H 7.31
					3.22	+0.02	2H 8.66
Leu-402	8.49	+0.07	4.39	+0.01	1.66	+0.01	γCH 1.66
					1.60	−0.05	δCH 0.92, 0.88
Gly-403	8.50	+0.11	3.98	+0.01			
			3.98	+0.01			
Gly-404	8.28	−0.11	4.00	+0.03			
			3.97	0			
Ala-405	8.23	−0.02	4.33	−0.02	1.37	−0.02	
Lys-406	8.35	−0.06	4.30	+0.06	1.86	+0.01	γCH 1.42, 1.42
					1.86	+0.10	δCH 1.69, 1.69
							εCH 3.03, 3.03
							εNH 7.62
Gln-407	8.36	−0.04	4.34	+0.07	2.09	−0.04	γCH 2.36
					1.98	−0.03	δNH (7.55), 6.83
Ala-408	8.40	+0.15	4.32	−0.03	1.40	+0.01	
Gly-409	8.38	−0.01	3.97	0			
			3.93	−0.04			
Asp-410	8.25	−0.16	4.80	−0.12	2.92	+0.08	
					2.82	+0.07	
Val-411	7.93	−0.51	4.18	0	2.13	0	γCH 0.93

[a] Condition: pH 3.0, 303 K, H_2O resonance at 4.86 ppm downfield from TSP. Assignments in parentheses are tentative. [b] Chemical shift differences: FGC 385–411 minus random-coil position (Bundi & Wüthrich, 1979).

$d_{\alpha N(i,i+2)}$ NOE between R391 and T393 could not be identified due to spectral overlap with the T393 βCH cross-peak.

A strong $d_{\alpha N}$ NOE between I394 and G395 in combination with the observation of a d_{NN} NOE between G395 and E396 and a $d_{\alpha N(i,i+2)}$ NOE between I394 and E396 suggests another β-turn from T393 to E396. The presence of other medium to large $d_{\alpha N}$ and d_{NN} NOEs within this segment is, at present, difficult to interpret. At best, this seems to be part of a multiple turnlike structure running from N390. On the other hand, the continuous series of d_{NN} NOEs running from I394 through H400 might suggest helical structure (Wüthrich, 1986); however, two observations tend to exclude this: (1) several large to medium sequential $d_{\alpha N}$ NOEs and (2) the absence of characteristic helical $d_{\alpha N(i,i3)}$ and $d_{\alpha\beta(i,i+3)}$ NOEs. The absence of NOEs by itself means little since NOEs can be greatly attenuated, for example, by increased motions/flexibility. Consistent with these data is a possible multiple-turn or irregular helical-type structure. This would then continue the two turns already suggested from N390 to E396. This anomalous segment seems to end in a turn from Q399 to L402. Medium $d_{\alpha N}$ H400 to H401 and d_{NN} H401 to L402 NOEs tend to support this.

The structural situation is less clear from G403 to V411. Throughout this segment, $d_{\alpha N}$ NOEs are generally smaller

Table II: ^{1}H NMR Sequence Assignments of the γ-Chain of Fibrinogen (12-mer)[a]

residue	NH	12–27[b]	αCH	12–27[b]	βCH	12–27[b]	others
His-400	8.86	+0.36	4.77	+0.15	3.31	+0.05	4H 7.40
					3.31	+0.16	2H 8.75
His-401	8.83	+0.23	4.86	+0.17	3.25	+0.02	4H 7.45
					3.25	+0.03	2H 8.74
Leu-402	8.61	+0.12	4.72	+0.33	1.80	+0.14	γCH 1.74
					1.74	+0.14	δCH 1.05, 0.90
Gly-403	8.49	−0.01	4.10	+0.12			
Gly-404	8.40	+0.12	4.12	+0.12			
Ala-405	8.48	+0.25	4.45	+0.12	1.55	+0.18	
Lys-406	8.46	+0.11	4.43	+0.13	1.98	+0.12	γCH 1.59, 1.59
					1.92	+0.06	δCH 1.84, 1.84
							εCH 3.17, 3.17
							εNH 7.71
Gln-407	8.45	+0.09	4.48	+0.14	2.25	+0.16	γCH 2.49
					2.13	+0.15	δNH 7.65, 6.98
Ala-408	8.35	−0.05	4.47	+0.15	1.52	+0.12	
Gly-409	8.59	+0.21	4.12	+0.15			
Asp-410	8.36	+0.11	4.91	+0.11	3.04	+0.12	
					2.94	+0.12	
Val-411	8.09	+0.16	4.39	+0.21	2.06	−0.07	γCH 1.05

[a] Conditions: pH 3.0, 303 K, H_2O resonance at 4.86 ppm downfield from TSP. [b] Chemical shift differences between FGC 400–411 and FGC 385–411.

than those in the N-terminal segment. No d_{NN} NOEs are observed. Observable $^3J_{\alpha N}$ coupling constants are around 6–7 Hz with the exception of V411 which has a value of about 10 Hz. A 6–7-Hz coupling constant is uninformative since no structural significance can be attributed. Three-bond J-coupling values are always averaged to 6.5–8 Hz for small peptides with fluctuating structures (Kessler & Bermel, 1986). Three out of nine possible d_{NN} cross-peaks were too close to the diagonal to be resolved. The presence of small $d_{\alpha N}$ NOEs and several 6–7-Hz $^3J_{\alpha H}$ values may suggest a highly fluctuating C-terminal conformation and/or lack of predominant structure from G403 and V411. Alternatively, chemical shift differences from random-coil positions (Bundi & Wüthrich, 1979) (Table I) suggest that some structure may exist. These chemical shift differences, unfortunately, are difficult to interpret. G403 NH gives a strong $d_{\alpha N}$ NOE to L402 αCH, and G404 NH chemical shifts, in particular, are significantly different from their random-coil positions, and their αCH_2 resonances are resolved from one another. Furthermore, chemical shifts of A408 NH, D410 NH, V411 NH, and D410 αCH are all significantly different from their random-coil positions. The geminal αCH_2 protons of G409 are also resolved from each other, and their NH resonance is shifted from most other glycine NH resonances, supporting the idea of a preferred C-terminal conformation.

C-Terminal Dodecapeptide. Since the C-terminal segment, residues 403–411, in FGC 385–411 evades secondary structure analysis, we chose to study the dodecapeptide FGC 400–411 and compare chemical shift differences with the parent chain. HOHAHA and NOESY spectra were acquired in H_2O, and sequential assignments in this smaller peptide were readily made by the approach described earlier. Overall, the αCH–NH fingerprint region appeared similar, but chemical shift differences were observed as listed in Table II. By maintaining the same solvent conditions for both peptides, such chemical shift comparisons can be informative when analyzed together with other data. Chemical shift differences, labeled "12–27" in Table II, should vary somewhat, especially when interresidue contact domains and regions of significant conformational variance are involved. Not all resonances respond equally to both factors, and it is difficult, therefore, to be definitive about the origins of these chemical shift changes. This approach is by no means infallible and must be viewed with caution due to the generally unpredictable behavior of chemical shifts. Many of these shift differences may be too small to be significant, but even if we assume a minimum meaningful significant shift difference of 0.1 ppm (Table II), several resonances are clearly affected. Large shift differences associated with proton resonances of H400 and H401 should not be considered since such shifts would be expected in newly created N-terminal residues. It was for this reason that this particular fragment was synthesized and shift differences of residues 402–411 could be more easily interpreted. For the remaining resonance, those belonging to protons of L402, G404, A405, K406, G409, D410, and V411 are particularly shifted. Moreover, in the dodecapeptide, G404 and G409 no longer exhibit nondegenerate αCH resonances (compare to Table I); just in passing, the H400 and H401 βCH and βCH′ resonances are now also degenerate. Qualitatively, therefore, these data suggest that some preferred conformation does indeed exist in the C-terminal segment of FGC 385–411. Conformational flexibility could explain why clear secondary structural elements could not be identified in NOESY data.

Long-Range NOEs. NOE data were also acquired at 30 °C with mixing times of 600 and 800 ms. No new d_{NN} NOEs were observed. At present, a number of weak long-range NOEs have been observed at shorter and longer mixing times among residues in the N-terminal domain, i.e., residues up to L402; none have been observed involving the C-terminal domain, i.e., residues 403–411. These long-range NOE data are currently being analyzed for use in distance geometry calculations. With the exception of Ala-405, $d_{\beta N(i,i)}$ NOEs have been observed, moreover, only for residues in the N-terminal domain. Several $d_{\beta N(i,i+1)}$ NOEs have also been observed only for residues in the N-terminal domain. These data support the idea of a fixed N-terminal domain structure and a more flexible, C-terminal segment. As mentioned earlier, the absence of long-range NOEs is not too surprising since distance cutoffs are more in the range of 3 Å instead of 4–5 Å found for more structurally constrained and/or larger proteins.

Long-Lived Backbone Amides. FGC 385–411 which had been lyophilized from H_2O solution and then dissolved in D_2O at pH 2.8, 25 °C, gives the proton NMR spectra shown in Figure 7. The lower spectrum acquisition was completed 10 min from the time of dissolution in D_2O, and the upper spectrum was taken after 30 min. This suggests that a number of backbone amides have half-life times of about 10–20 min under these conditions. The well-resolved C-terminal V411

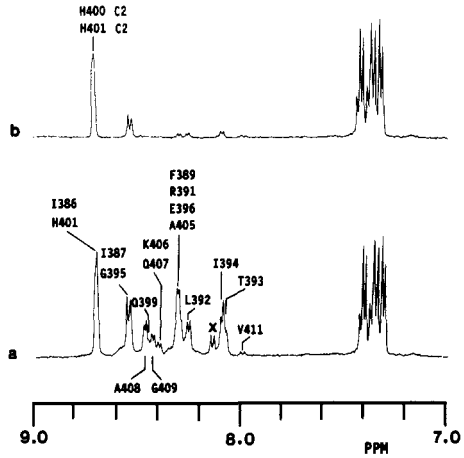

FIGURE 7: Long-lived amides in FGC 385–411. Two conventional proton NMR spectra are shown for H_2O-exchanged, lyophilized FGC 385–411 in D_2O/20 mM potassium phosphate, pH 2.8, 25 °C. The lower spectrum was completed within 10 min after dissolving in D_2O; the upper spectrum was taken after about 30 min. Residues are labeled above their approximate NH resonance positions.

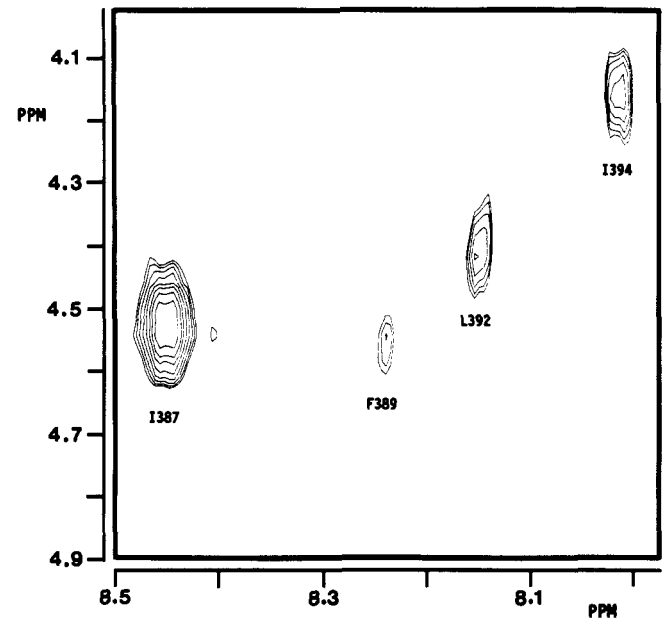

FIGURE 8: COSY contour plot identifying long-lived amides. A COSY contour plot is shown for H_2O-exchanged, lyophilized FGC 385–411 in D_2O/20 mM potassium phosphate, pH 2.8, 10 °C. The 2D NMR data were acquired within 4 h after dissolving the peptide powder in D_2O. Total of 256 t_1 time-incremented 1K data point FIDs (32 scans each) were accumulated and processed as described in the Figure 1 legend.

NH, for example, exchanges very rapidly as might be expected for a terminal residue. Some long-lived amides could be identified on the basis of their chemical shifts, while others could not. Figure 7 indicates the approximate chemical shifts of long-lived NHs. Aside from V411, backbone NH resonances belonging to L392, T393, and I394 could be identified based solely on their unambiguous chemical shifts. The region between 8.42 and 8.29 ppm also allows identification of NH resonances for residues 399, 406/407, 408, and 409; of these, the NHs of 406/407 and 409 exchange more rapidly. The C-terminal A408 NH, interestingly, does have a respectable half-life, supporting the idea of a preferred C-terminal structure. The A408 NH, moreover, is one of the most highly shifted resonances from its random-coil position (Table I) and exhibits a $^3J_{\alpha N}$ value of 5 Hz which is outside the range of $^3J_{\alpha N}$ values observed for highly fluctuating peptide structures (Kessler & Bermel, 1986). A previously unobserved NH resonance (labeled "x", Figure 7a) is present under these conditions. The only unassigned NH resonances belong to the K385 backbone NH_2, and the N390 δNH_2. To be so far downfield-shifted, this NH resonance either must belong to the K385 backbone NH_2 or be involved in a hydrogen bond. The K385 backbone NH_2 is perhaps the more logical choice.

Identity of the longest lived amides was made by performing a COSY experiment at lower temperature to extend NH lifetimes. A COSY spectrum taken at 10 °C, for instance, shows the presence of four αCH–NH cross-peaks (Figure 8) which could be identified as belonging to I387, F389, L392, and I394. In this small peptide, relatively long-lived NHs might be expected for residues involved in H-bonded structures. T393, for example, is proposed to occupy position 4 of a β-turn; its probably H-bonded NH, therefore, might be expected to be relatively long-lived although it is less long-lived than any of these four. Surprisingly, I387 NH at the N-terminus is the longest lived of all backbone NHs in the peptide. L392 and I394 are proposedly involved in positions 3 and 2, respectively, of β-turns, while F389, like I387, is part of an extended-chain conformation. As yet, it is unknown why these backbone amides are so long-lived.

Discussion

Generally, small peptides in solution do not maintain a well-defined conformation but rather exist as an ensemble of highly fluctuating structures. In certain peptides, however, it is possible to find one dominant solution conformation. Reed et al. (1988), for example, recently found a dominant solution conformation of "nested β-bends" for the fibronectin-derived hexapeptide GRGDSP. In FGC 385–411, only the C-terminal segment, residues 403–411, remains structurally nondiscript. The N-terminal segment from residues 385–403, on the other hand, shows numerous strong $d_{\alpha N}$ NOEs, $^3J_{\alpha N}$ coupling constants of 9–10 Hz, a continuous run of d_{NN} NOEs from residues 394–400 in addition to two d_{NN} NOEs between L392-T393 and H401-L402, and several relatively long-lived amide protons. At the very least, these data suggest the presence of a dominant solution conformation within this domain.

K385, I386, and I387 seem to adopt an extended-chain conformation. A backbone "kink" at trans-P388 interrupts this structure. A probable β-turn from N390 to T393 begins what is perhaps best described as a multiple-turn conformation ending at about L402. A β-turn contains four residues and is typified, for example, with β-turn type II, by a relatively large $d_{\alpha N}$ NOE between residues 2 and 3 and a d_{NN} NOE between residues 3 and 4 (Wüthrich, 1986). The string of d_{NN} NOEs, combined with the observation of relatively large $d_{\alpha N}$ NOEs, suggests that this multiple-turn conformation may contain elements of left-handed, α-helix structure. The left-handed, α-helix is, in any event, no more than a continuous series of deformed type II β-turns. Although clearly defined as a favorable peptide backbone conformation in Ramachandran ϕ,ψ phase space (Dickerson & Geis, 1969), left-handed α-helices have not been observed in globular proteins studied to date. Fibrinogen, however, is in the class called fibrous proteins about which limited structural information is available. More specific structural information will have to await time-dependent NOESY and rotating-frame NOESY (Bax & Davis, 1985) experiments and distance geometry/energy minimization calculations.

Long-lived amide protons have been observed at several backbone NH positions throughout the N-terminal segment as indicated in Figure 6. Two reasons are normally given to explain the presence of long-lived amides (Englander et al.,

1972): (1) buried within the protein matrix and (2) hydrogen bonded in a well-defined structure. The former explanation seems inapplicable in this case of a small protein containing only 27 residues. The latter explanation is, therefore, more reasonable and supports the idea of a well-defined, dominant N-terminal solution conformation in FGC 385–411. The presence of multiple β-turns could explain the observation of these relatively long-lived, probably hydrogen-bonded, backbone amide protons observed throughout this domain. At present, however, it is unclear why the longest lived amide, belonging to I387, exists in a probable extended-chain structure. If anything, peptide termini tend to be more flexible and not less as is the case at hand. The turns at N390–T393–E396 place E396 in proximity to the N-terminal K385 residue for a possible stabilizing interresidue salt bridge. Although the proposal of such a salt bridge is speculative, something giving added inflexibility or stability to the N-terminus must be present in order to account for the relatively longest lived I387 backbone amide proton. Other amide protons involved in proposed β-turns, for example, are less long-lived.

The remaining portion of the peptide, residues 403–411, is structurally less well-defined. Significant chemical shift deviations from random-coil positions, while giving no specific evidence for a particular conformation, suggest the existence of some preferred structure. This proposal is supported by significant chemical shift differences in the dodecapeptide FGC 400–411 when compared to FGC 385–411. The absence of d_{NN} NOEs and the presence of 6–7-Hz $^3J_{\alpha N}$ coupling constants, however, leave considerable room for a multitude of possible conformations. Conformational energy calculations indicate that the sequence X-Gly-Gly-Y has a high probability for β-bend formation (Zimmerman & Scheraga, 1978). It has also been reported that this sequence often exists as a β-turn in proteins (Sibanda & Thornton, 1985). Such a sequence is present in FGC 385–411 with L402, G403, G404, and A405. Significant chemical shift differences between FGC 385–411 and FGC 400–411 have been noted for G404 and A405. Moreover, the resolution of individual αCH resonances for G404 observed in FGC 385–411 is lost in the shorter fragment. Clear evidence, however, is lacking in our data to prove the presence of a β-turn. The d_{NN} NOE normally observed between positions 3 and 4 in a β-turn is not observed; moreover, since two glycine residues would occupy positions 2 and 3 of such a turn, $d_{\alpha N}$ NOE magnitudes are unclear. If such a turn did exist within this segment, it would continue the trend of multiple turnlike structure previously noted. Conformational flexibility in this C-terminal segment is perhaps the best explanation for lack of NMR structural data.

Similar NMR structural studies have been performed on a fibrinogen peptide from the Aα-chain of human fibrinogen, residues 1–23 (Ni et al., 1988). This fibrinogen α-chain fragment contains a relatively flexibile N-terminal segment, i.e., residues 1 to about 10, and a more structured C-terminal segment. Interestingly, the dominant C-terminal structural feature is β-turn as in the present case for FGC 385–411. On the basis of the Chou–Fasman secondary structure predictive algorithm, fibrinogen chains should possess mostly aperiodic and turn structural elements (Jollès et al., 1978). At least with these two examples of small fibrinogen peptides, this is the case.

Based primarily on tryptic digestion and amino acid sequencing studies on human and bovine cross-linked fibrins, Chen and Doolittle (1971) proposed that Q398 and K406 are interresidue cross-linked [ε-(γ-glutamyl)lysine] between two opposing fibrinogen γ-chains. Doolittle (1973) later proposed that the L392–V411 segment exists in an α-helical conformation so that Q398 and K406 would lie on the same side of antiparallel running helices in the two linked γ-chains. Our NMR structural data show that, at least with the γ-chain 385–411 C-terminal fragment, aspects of the appealing, modeled helical segment may exist. A multiple turn-like structure running from N390 through to K406 could also allow Q398 and K406 to face the same direction for interchain cross-linking.

The fibrinogen domain recognizing receptors on ADP-activated human platelets is located in the C-terminal domain of FGC 385–411, i.e., residues 400–411 (Kloczewiak et al., 1984). Penta- and hexapeptides from this fragment are much less active, suggesting that the dodecapeptide folding pattern and/or sequence influences normal activity. Amino acid substitutions at various positions in the C-terminal dodecapeptide have pronounced, detrimental effects on this fragment's reactivity toward these platelet receptors (Kloczewiak et al., 1988). While we cannot specifically reason why any one such substitution would attenuate activity, the secondary structure of the 27-residue C-terminal fragment as indicated here does suggest that residues 403–411 possess a less well-defined, perhaps relatively more flexible, conformation than the N-terminal portion of the peptide. Such a nonregular structure may be more prone to conformational changes induced by the substitution of any one amino acid residue. Interestingly, only substitution of A408 in FGC 400–411 with arginine significantly enhances biological activity of FGC 400–411 (Kloczewiak et al., 1988). In fact, shorter, fibrinogen-derived peptides AKQ*RGD*F and KQ*RGD*F (RGD in place of AGD) are more active than the parent fragment 400–411 (Timmons et al., 1989). This may not be too surprising since the tripeptide RGD has been recognized as playing a critical role in cell recognition and adhesion (Ruoslahti & Pierschbacher, 1987). The NMR solution conformation of a related hexapeptide sequence derived from another fibrous protein, fibronectin, i.e., G*RGD*SP, which contains the RGD tripeptide sequence, shows the existence of "nested β-turn" structure (Reed et al., 1988). The biologically interesting fibrinogen γ-chain, C-terminal KQ*AGD*V sequence does seem to possess some type of preferred conformation, although, at this point, it is impossible to identify the type. Amidation of the C-terminus carboxylate or substitution of V411 for even a similar, hydrophobic residue, i.e., leucine, causes a significant decrease in platelet receptor reactivity (Kloczewiak et al., 1989). The apparent flexibility of the FGC 385–411 C-terminus may be necessary to probe the conformational binding space at the receptor. A specific conformation may be "locked-in" upon receptor binding. By using transferred NOE experiments, Ni et al. (1989) have observed such a stabilized conformational state in the Aα-chain segment 1–23 bound to thrombin. It would be interesting to try similar experiments with FGC 385–411 or FGC 400–411 and its platelet receptor.

References

Aue, W. P., Bartholdi, E., & Ernst, R. R. (1976) *J. Chem. Phys. 64*, 2229–2246.

Barany, G., & Merrifield, R. B. (1980) in *The Peptides: Analysis, Synthesis, Biology* (Gross, E., & Meienhofer, J., Eds.) Vol. 2, pp 1–284, Academic Press, New York.

Bax, A., & Davis, D. G. (1985) *J. Magn. Reson. 63*, 207–213.

Blomback, B., & Yamashina, I. (1958) *Ark. Kemi 12*, 299–310.

Bundi, A., & Wüthrich, K. (1979) *Biopolymers 18*, 285–298.

Chen, R., & Doolittle, R. F. (1969) *Proc. Natl. Acad. Sci. U.S.A. 63*, 420–426.

Chen, R., & Doolittle, R. F. (1970) *Proc. Natl. Acad. Sci. U.S.A. 66*, 427–479.

Chen, R., & Doolittle, R. F. (1971) *Biochemistry 10*, 4486–4491.

Chou, P. Y., & Fasman, G. D. (1978) *Adv. Enzymol. Relat. Areas Mol. Biol. 48*, 45–148.

Davis, D. G., & Bax, A. (1985) *J. Am. Chem. Soc. 107*, 2820–2821.

Dickerson, R. E., & Geis, I. (1969) *The Structure and Action of Proteins*, Harper & Row, New York.

Doolittle, R. F. (1973) *Adv. Protein Chem. 27*, 1–109.

Englander, S. W., Downer, N. W., & Teitelbaum, H. (1972) *Annu. Rev. Biochem. 41*, 903–924.

Jeener, J., Meier, B. H., Bachmann, P., & Ernst, R. R. (1979) *J. Chem. Phys. 71*, 4546–4553.

Jollès, P., Loucheux-Lefevre, M., & Henschen, A. (1978) *J. Mol. Evol. 11*, 271–277.

Kessler, H., & Bermel, W. (1986) in *Methods in Stereochemical Analysis 6*: *Applications of NMR Spectroscopy to Problems in Stereochemistry and Conformational Analysis* (Takenchi, Y., & Marchand, A. P., Eds.) VCH, Deerfield Beach, FL.

Kloczewiak, M., Timmons, S., & Hawiger, J. (1982) *Biochem. Biophys. Res. Commun. 107*, 181–187.

Kloczewiak, M., Timmons, S., Lukas, T. J., & Hawiger, J. (1984) *Biochemistry 23*, 1767–1773.

Kloczewiak, M., Timmons, S., Bednarek, M., Sakon, M., & Hawiger, J. (1989) *Biochemistry 28*, 2915–2919.

McKee, P. A., Mattock, P., & Hill, R. L. (1970) *Proc. Natl. Acad. Sci. U.S.A. 66*, 738–744.

Ni, F., Scheraga, H. A., & Lord, S. T. (1988) *Biochemistry 27*, 4481–4491.

Ni, F., Konishi, Y., Frazier, R. B., Scheraga, H. A., & Lord, S. T. (1989) *Biochemistry 28*, 3082–3094.

Piantini, U., Sørensen, O. W., & Ernst, R. R. (1982) *J. Am. Chem. Soc. 104*, 6800–6805.

Reed, J., Hull, W. E., von der Lieth, C.-W., Kübler, D., Suhai, S., & Kinzel, V. (1988) *Eur. J. Biochem. 178*, 141–154.

Ruggeri, Z. M., Houghten, R. A., Russel, S. R., & Zimmerman, T. S. (1986) *Proc. Natl. Acad. Sci. U.S.A. 83*, 5708–5711.

Shaka, A. J., & Freeman, R. (1983) *J. Magn. Reson. 51*, 161–169.

Sibanda, B. L., & Thornton, J. M. (1985) *Nature (London) 316*, 170–174.

States, D. J., Haberkorn, R. A., & Ruben, D. J. (1982) *J. Magn. Reson. 48*, 286–293.

Timmons, S., Bednarek, M. A., Kloczewiak, M., & Hawiger, J. (1989) *Biochemistry 28*, 2919–2923.

Wider, G., Macura, S., Anil-Kumar, Ernst, R. R., & Wüthrich, K. (1984) *J. Magn. Reson. 56*, 207–234.

Wüthrich, K. (1986) *NMR of Proteins and Nucleic Acids*, Wiley-Interscience, New York.

Zimmerman, S. S., & Scheraga, H. A. (1978) *Biopolymers 17*, 1871–1885.